Eur Radiol (2004) 14:409–416
DOI 10.1007/s00330-003-2176-1

CARDIAC

Peter Hunold
Stefan Maderwald
Holger Eggebrecht
Florian M. Vogt
Jörg Barkhausen

Steady-state free precession sequences in myocardial first-pass perfusion MR imaging: comparison with TurboFLASH imaging

Received: 24 March 2003
Revised: 27 October 2003
Accepted: 3 November 2003
Published online: 26 November 2003

P. Hunold (✉) · S. Maderwald
F. M. Vogt · J. Barkhausen
Department of Diagnostic
and Interventional Radiology,
University Hospital Essen,
Hufelandstrasse 55, 45122 Essen, Germany
e-mail: peter.hunold@uni-essen.de
Tel.: +49-201-7231527
Fax: +49-201-7231563

H. Eggebrecht
Department of Cardiology,
Center of Internal Medicine,
University Hospital,
Essen, Germany

Abstract The aim of this study was to compare the image quality of a saturation-recovery gradient-recalled echo (GRE; TurboFLASH) and a saturation-recovery SSFP (SR-TrueFISP) sequence for myocardial first-pass perfusion MRI. Eight patients with chronic myocardial infarction and 8 volunteers were examined with a TurboFLASH (TR 2.1 ms, TE 1 ms, FA 8°) and a SR-TrueFISP sequence (TR 2.1 ms, TE 0.9 ms, FA, 50°) on a 1.5 T scanner. During injection of 0.05 mmol/kg BW Gd-DTPA at 4 ml/s, three short axis slices (8 mm) of the left ventricle (LV) were simultaneously scanned during breath-hold. Maximum signal-to-noise ratio (SNR), contrast-to-noise ratio (CNR) between infarcted and normal myocardium, and percentage signal intensity change (PSIC) were measured within the LV lumen and in four regions of the LV myocardium for the three slices separately. For the LV lumen, SR-TrueFISP was superior in SNR and PSIC (factor 3.2 and 1.6, respectively). Mean maximum SNR, PSIC, and CNR during peak enhancement in the LV myocardium were higher for SR-TrueFISP compared with TurboFLASH (factor 2.4, 1.25, and 1.24, respectively). The SNR was higher in the septal portion of the ventricle than in anterior/posterior and lateral regions. The SR-TrueFISP provides higher SNR and improves image quality compared with TurboFLASH in first-pass myocardial perfusion MRI.

Keywords MRI · Ischemic heart disease · Myocardium

Introduction

A decrease in myocardial perfusion will be the first effect of occluding coronary artery disease (CAD) and can be detected before clinical symptoms or left ventricular (LV) dysfunction become obvious; therefore, the assessment of myocardial perfusion representing the functional relevance of coronary stenoses appears the most promising concept for a non-invasive test to detect CAD. To date, nuclear techniques, i.e., single photon emission computed tomography (SPECT) and positron emission tomography (PET), serve as the reference standard in this respect [1]. For the detection of significant CAD, these techniques provide a sensitivity and specificity of 83–95% and 53–95%, respectively [2, 3, 4]. They are, however, limited by attenuation artifacts, radiation exposure, and a poor spatial resolution which does not allow the reliable detection of subendocardial perfusion defects.

Perfusion MRI using the first-pass kinetics of a bolus of gadolinium-based contrast agent has been developed to overcome the nuclear techniques' difficulties and limitations [5, 6]. In this context, different sequences have been evaluated and proven feasible [7, 8, 9, 10]; however, most of the recent studies have been performed using fast gradient-echo sequences such as TurboFLASH with either inversion- [8] or saturation-recovery techniques [11, 12]. Steady-state free precession (SSFP) sequences have been successfully applied in cardiac MRI for functional studies [13, 14] and coronary angiography [15]. They have been proven to provide high signal-to-noise ratio (SNR) and

high contrast-to-noise ratio (CNR), and to shorten acquisition time compared with gradient-echo sequences.

The contrast of steady-state free precession sequences depends on the T2/T1 properties of the tissue; however, using an inversion pulse combined with the ultra-fast data readout of the steady-state free precession sequence, predominantly T1-weighted images can be obtained. Alternatively, T1-weighting can be enhanced by adding saturation pulses, which seem to be well suited for myocardial perfusion imaging.

The purpose of the present study was to compare the SNR, CNR, and the signal intensity (SI) increase of a fast saturation-recovery GRE (TurboFLASH) and a saturation-recovery SSFP (TrueFISP) sequence for myocardial first-pass perfusion MRI.

Materials and methods

In this study 8 patients and 8 young healthy volunteers (6 men and 2 women; mean age 25±2 years) were enrolled. Eight patients (5 men and 3 women; mean age 62±9 years) had CAD proven by catheter coronary angiography and a history of chronic myocardial infarction. Data on the patients' individual history of myocardial infarction, current status of CAD as visually assessed, present LV function, and delay between infarction and imaging are given in Table 1. Written informed consent was acquired from all subjects, and the study was performed in accordance with the regulations of the institutional review board.

MRI

All MRI examinations were performed on a 1.5 T whole body scanner (Magnetom Sonata, Siemens Medical Systems, Erlangen, Germany) equipped with high-performance gradients (maximum amplitude, 40 mT/m; slew rate 200 T/m s^{-1}). Patients were placed in supine position. Two coil elements of the CP spine array and two elements of the conventional body flex phased-array coil were used for signal reception.

MRI technique

In each subject, two myocardial first-pass studies were performed with at least 24 h (mean time interval 3.1 days, range 28 h to 12 days) in between using either TurboFLASH or TrueFISP with saturation-recovery preparation in random order. For determination of the proper short axis orientation, a cine study was obtained in horizontal and vertical long-axis orientation using a segmented steady-state free precession (SSFP) sequence (TrueFISP; TR 3.0 ms, TE 1.5 ms, flip angle 60°, bandwidth 975 Hz per pixel). Based on these images, the ECG-triggered multi-slice perfusion study was performed in short-axis orientation while contrast material was injected. Scan parameters of both perfusion sequences are given in Table 2. During breath hold for a period of 40 heart beats, 3 parallel slices were simultaneously obtained in the basal, midventricular, and apical position of the LV. After completion of the first perfusion study, a segmented inversion recovery (IR) TurboFLASH sequence was applied as described elsewhere [16] to detect late enhancement and characterize myocardial scarring in the acquired short-axis slices.

Contrast material injection protocol

During imaging, 0.05 mmol/kg BW of Gd-DTPA (Magnevist, Schering, Berlin, Germany) at a flow rate of 4 ml/s were injected through an 18-G cannula in an antecubital vein followed by a 20 ml flush of saline. An automated injector pump (Spectris, Medrad Inc., Indianola, Pa., USA) was used. After that, an additional 0.15 mmol/kg BW of Gd-DTPA was administered for the late enhancement study.

Data analysis

All perfusion data sets of the three reference slices were evaluated by an experienced board-certified radiologist.

Table 2 Scan parameters for saturation-recovery TurboFLASH and saturation-recovery TrueFISP sequences used for myocardial first-pass perfusion MR imaging in this study

	TurboFLASH	TrueFISP
TR (ms)	2.1	2.1
TE (ms)	1.0	0.9
Flip angle (°)	8	50
Bandwidth (Hz/pixel)	770	1400
Matrix	128×80	128×77
Spatial resolution (mm^2)	3.9×3.1	4.0×3.1

Table 1 Patient data on individual history of chronic myocardial infarction concerning date and target vessel, current status of coronary artery disease (vessel and stenosis degree), present global left ventricle function (EF), and delay between infarction and MR imaging. *LAD* left anterior descending, *RCA* right coronary artery, *CAD* coronary artery disease, *CABG* coronary artery bypass graft

Patient no.	Gender	Age (years)	Myocardial infarction		Delay (months)	CAD status	Ejection fraction (%)
			Time (month/year)	Vessel			
1	F	63	6/2000	LAD	13	No stenosis	36
2	M	43	3/2001	LAD	12	No stenosis	43
3	M	73	8/1999	RCX	23	LAD and RCX occluded, 2 CABG	31
4	F	58	10/2001	LAD	5	LAD 60%, RCA 70%	35
5	M	67	7/1998	RCA, RCX	43	RCX 60%, LAD 75%	43
6	F	71	3/2000	LAD	24	LAD 50%	38
7	M	64	12/1999	RCX	26	RCX occluded, LAD 75%	29
8	M	60	3/1998	RCA	47	LAD 50%, RCA 75%	32
Mean±SD		62±9			24±15		36±5

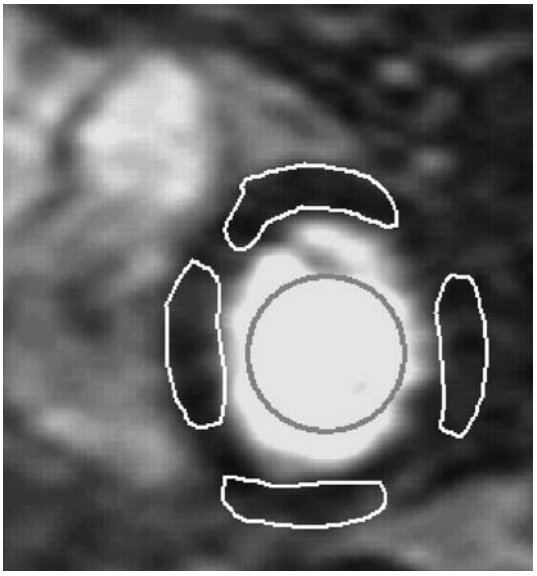

Fig. 1 Short-axis slice of the basal left ventricle (LV) during peak enhancement using the TurboFLASH sequence. Four regions of interest (ROIs) are placed within the LV myocardium in anterior, septal, inferior, and lateral position. Another circular ROI is put in the LV cavity to measure the LV input function

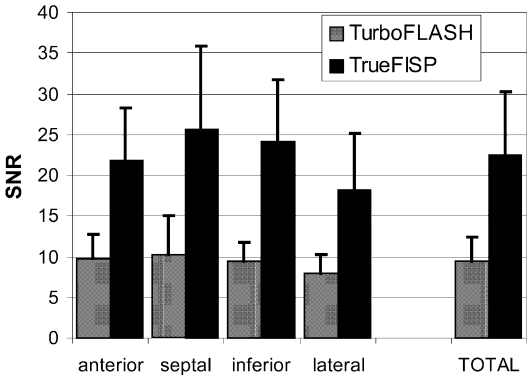

Fig. 2 Mean signal-to-noise ratio (SNR) measured in four different segments (ROIs) within three slices of the LV myocardium in all subjects with TurboFLASH (*gray bars*) and TrueFISP (*black bars*). The difference was significant in each comparison ($p<0.001$)

Signal-to-noise ratio

Signal-to-noise ratio (SNR) was calculated for four myocardial segments in each of the three LV slices as well as for the LV cavity at the individual time of maximum contrast enhancement. For these purposes, the mean signal intensities (SI) in four regions of interest (ROIs) of approximately 1 cm^2 were measured within the LV myocardium at the anterior, septal, inferior, and lateral positions (Fig. 1). Care was taken to not include blood or epicardial fat in the ROI. For measuring the blood pool SNR within the LV lumen, a circular ROI was set centrally excluding the papillary muscles and the myocardial wall (Fig. 1). The SNR was calculated by using the following standard formula: SNR=SI/noise [17]. Noise was defined as the standard deviation (SD) of mean SI in a ROI set in an artifact-free region outside the subject.

Contrast-to-noise ratio

For contrast-to-noise ratio (CNR) evaluation between myocardial scar after infarction and normal myocardium, the SI within the scar (SI_{scar}) as characterized by late enhancement imaging and one adjacent region of normal myocardium (SI_{myo}) were measured in all patients. Noise was again defined as the SD of mean SI in a ROI set outside the subject. The CNR was calculated following the standard equation: $CNR=(SI_{myo}-SI_{scar})/noise$.

Percentage signal intensity change

The percentage signal intensity change (PSIC) was evaluated in all ROIs within the myocardium and the LV lumen corresponding to the SNR measurements. The PSIC was calculated dividing the maximum signal intensity in each individual ROI by the signal intensity before contrast enhancement.

Statistical analysis

The SPSS (Version 11.0 for Windows, SPSS, Chicago, Ill.) statistics package was used. Comparison between the measured SNR, CNR, and PSIC data was done by using the paired *t* test. Differences between patients and volunteers were evaluated using the unpaired *t* test. *p* values <0.01 were considered to indicate a significant difference. Not significant results were designated by "n.s.".

Results

All data sets provided sufficient image quality. In each patient 12 ROIs were analyzed for the myocardium and 3 for the LV cavity for both TurboFLASH and TrueFISP images.

Signal-to-noise ratio

Measuring in all LV myocardial segments, mean SNR in TurboFLASH and TrueFISP was 9.4±3.1 and 22.4±7.8 ($p<0.001$), respectively. Figure 2 shows the comparison of SNR based on the different myocardial segments. For TurboFLASH, SNR in the anterior, septal, inferior, and lateral segment was 9.7±3.1, 10.3±4.7, 9.4±2.3, and 8.0±2.3. For TrueFISP, it was 21.9±6.3, 25.7±10.1, 24.1±7.7, and 18.1±7.1 ($p<0.001$ in each comparison). In total, TrueFISP yielded a 2.4-fold higher SNR in comparison with TurboFLASH.

In both sequences, SNR was higher in septal (TurboFLASH and TrueFISP, 10.3 and 25.7) than in anterior (9.6, 22.1), inferior (9.8, 24.1), and lateral (8.0, 18.1) segments ($p<0.001$ in each comparison). Concerning all investigated segments, higher SNR was found in the apical portion of the ventricle (TurboFLASH and TrueFISP,

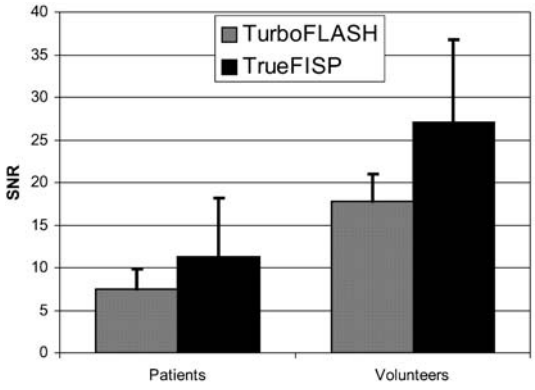

Fig. 3 Comparison of mean SNR measured in all ROIs between patients and volunteers. Significant differences were found between patients and volunteers in both techniques, as well as between TurboFLASH and TrueFISP, in both groups

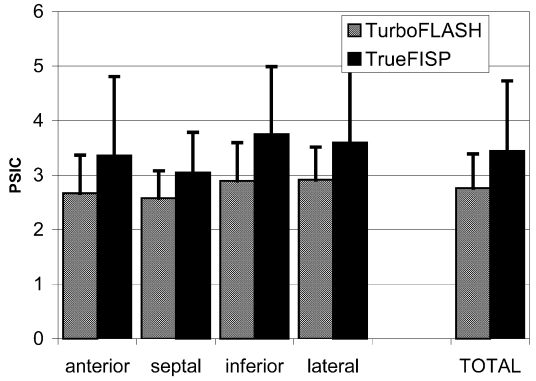

Fig. 4 Percentage signal intensity change measured in four different segments (ROIs) within three slices of the LV myocardium in all subjects with TurboFLASH (*gray bars*) and TrueFISP (*black bars*). The differences in each compared segment, as well as the total comparison, were not significant (n.s.)

9.8 and 27.0) than in the mid-ventricular (9.4, 21.1) and in the basal (9.1, 19.4) portions ($p<0.001$ in each comparison). In total, the volunteers tended to higher SNR than the patients in both TurboFLASH (11.3±3.2 vs 7.4±2.4, n.s.) and TrueFISP sequences (27±9.7 vs 17.8±6.8, n.s.; Fig. 3).

The SNR measured within the LV cavity (blood pool) was 3.2-fold higher for TrueFISP than for TurboFLASH (100.6±32.7 vs 31.3±8.4, $p<0.001$). Visually, all TrueFISP images appeared less noisy than the TurboFLASH images and, thus, provided subjectively better image quality.

Contrast-to-noise ratio

In the patient group the CNR measurements between scar and normal myocardium showed higher values for TrueFISP compared with TurboFLASH. The CNR in TurboFLASH and TrueFISP ranged from 1.5 to 10.1 and 1.8 to 14.2, respectively. Comparing the single measurements in each patient, the mean benefit in CNR using TrueFISP was 24%±12 (range 6–41%, $p<0.01$).

Percentage signal intensity increase

Measuring the PSIC over all LV myocardial segments, TrueFISP tended to higher PSIC than TurboFLASH (3.4±1.3 vs 2.8±0.6, n.s.). Figure 4 shows the comparison of PSIC for the different myocardial segments. For TurboFLASH, PSIC in the anterior, septal, inferior, and lateral segment was 2.7±0.7, 2.6±0.5, 2.9±0.7, and 2.9±0.6. For TrueFISP, values were 3.4±1.4, 3.0±0.5, 3.8±1.2, and 3.6±1.7 (n.s. concerning individual sequence comparison).

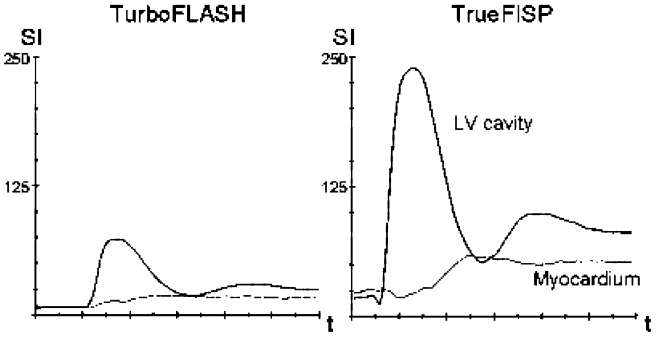

Fig. 5 Original signal–time curves of TurboFLASH (*left*) and TrueFISP (*right*) measured within the LV cavity ("input function", *upper lines*) and an anterior segment (*lower lines*) of a volunteer. Scaling of the y-axis is the same in both graphs. Significantly higher up-slopes for blood pool and myocardial signal intensity in the TrueFISP curves are obvious (99 vs 34 and 5.6 vs 1.14 SI/hb, respectively)

When measuring PSIC of the blood pool by the ROI within the LV cavity, again, TrueFISP yielded higher values than TurboFLASH: 15.5±4.9 vs 9.8±2.3 (factor 1.6, $p<0.001$). Figure 5 shows the signal intensity–time curves of the myocardium and the blood pool for both TurboFLASH and TrueFISP sequences in a volunteer.

Patients vs volunteers

Volunteers tended to higher SNR than patients during peak enhancement in both TurboFLASH and TrueFISP (11.3±3.2 vs 7.4±2.4, n.s.; Fig. 3). In both groups, TrueFISP yielded higher SNR than TurboFLASH (17.8±6.8 vs 7.4±2.4 in patients, $p<0.05$; 27±9.7 vs 11.3±3.2 in volunteers, $p<0.01$).

Discussion

In the present study, saturation-recovery TrueFISP techniques in myocardial first-pass perfusion MRI have been shown to provide better image quality and higher SNR when compared with the established gradient-echo sequences such as TurboFLASH. Furthermore, significantly higher CNRs between infarcted and normal myocardium are provided by TrueFISP.

Comparison between TurboFLASH and TrueFISP

In our study examining volunteers and patients after infarction, the same field of view and very similar spatial and temporal resolution (effective temporal resolution, 168 vs 191 ms) were used for both TurboFLASH and TrueFISP sequences in a multi-slice approach. Under these premises, True FISP provided significantly higher SNR and CNR than did TurboFLASH (Fig. 2). Furthermore, when visually assessed, TrueFISP looked remarkably less noisy.

When SSFP myocardial perfusion imaging was first described in an animal experiment by Schreiber et al. in 2001, it was proven to provide high image quality in combination with high spatial resolution [18]. The same group reported another study in phantoms and healthy volunteers comparing single-slice saturation-recovery TurboFLASH and TrueFISP perfusion sequences finding significantly higher spatial resolution of the TrueFISP when maintaining comparable SNR [19]. That, of course, implements higher SNR and CNR when the same voxel size is used. Corresponding to our results, the authors also reported the impression of less noisy images using TrueFISP when comparing qualitatively. Another important finding of the mentioned study [18] in terms of the reliability of True FISP measurements is the linearity of signal intensity at a wide range of contrast material concentration.

Comparing the scan parameters of TurboFLASH and TrueFISP (Table 2), the TrueFISP technique uses remarkably higher flip angles. The capabilities of GRE sequences, such as TurboFLASH, might, theoretically, be enhanced by higher flip angles to obtain higher signal warranting higher SNR and CNR. However, higher flip angles than the given are accompanied by saturation effects, which prohibit their application; thus, parts of the TrueFISP advantages, in terms of SNR and CNR, are based on the opportunity to use higher flip angles.

As a prerequisite of the delineation of ischemic areas within the myocardium, a wide range of signal intensity between the precontrast images and the peak enhancement should be provided. As a measure of the achievable distinction between ischemic and normally perfused myocardium comparing TurboFLASH and TrueFISP, we assessed the PSIC. The finding that TrueFISP is superior in this topic very closely matches the data published by Schreiber et al. and is of the same order of magnitude [19]; however, the difference did not reach statistical significance in this small number of subjects. Visually, the distinction of certainly hypoperfused areas, i.e., infarction zone, in the patient portion of our study was easier in TrueFISP (Figs. 6, 7), yet we could not confirm this impression by CNR measurements due to the lack of a reference standard, in terms of perfusion, such as PET or SPECT.

In conclusion, TrueFISP allows for a more distinct delineation between normal and chronically infarcted myocardium; however, in the clinical setting of CAD assessment, the most important issue is the differentiation between normally perfused myocardium and perfusion deficits in viable myocardium. An improvement in this topic by using TrueFISP sequences may be suggested from the quantitative CNR measurements we presented, although further studies have to be performed to clarify the differences between the two mentioned techniques in this respect.

Use of prepulses

Using T1-shortening contrast agents for myocardial perfusion MRI, the utilized sequences have to warrant T1-weighting as much as possible. In SSFP studies for myocardial function and coronary angiography, the intrinsic "T2-like" contrast is used. To make SSFP suitable for contrast agent applications, prepulses have to be added. Either IR or saturation-recovery prepulses may be used. Although IR sequences provide stronger T1-weighting, they are much more vulnerable to artifacts through triggering difficulties in arrhythmias. Moreover, IR prepulses prolong the acquisition times, which is disadvantageous in multi-slice scanning; therefore, SR prepulses are mostly used in the particular field of myocardial perfusion imaging.

Signal inhomogeneity

Our data show that there is a significant difference in mean SNR between the different myocardial areas using either TurboFLASH or TrueFISP. Corresponding to the study published by Muhling et al. [20], the septal portion of the ventricle provided the highest SNR values compared with the lateral and inferior segments. This is due to the proximity of the body array coil, which is positioned on the subject's chest, to the anteroseptal segments. The resulting signal inhomogeneity accounts for less signal in the dorsal parts of the body. This is of importance when a quantitative data analysis of the perfusion is performed and it warrants normalization of the measured maximum signal intensity to the precontrast images for each individual segment.

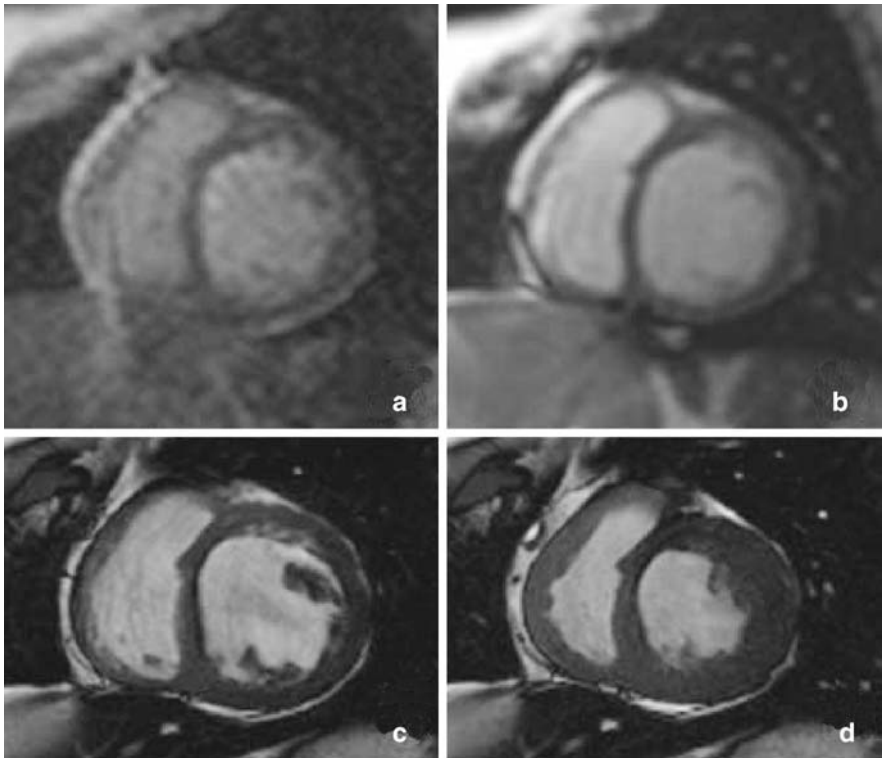

Fig. 6a–d Short-axis scan of a basal to mid-ventricular slice of a patient with a history of septal myocardial infarction. First-pass perfusion imaging (*top row*) with **a** TurboFLASH and **b** TrueFISP. A perfusion deficit may be appreciated in the anteroseptal segment which is better delineated by TrueFISP. Note the remarkably higher noise in the TurboFLASH image. The *bottom row* shows Cine SSFP images in **c** end-iastole and **d** end-systole with an akinesia in the corresponding anterior portion of the septum and a hypokinesia in the inferior septum

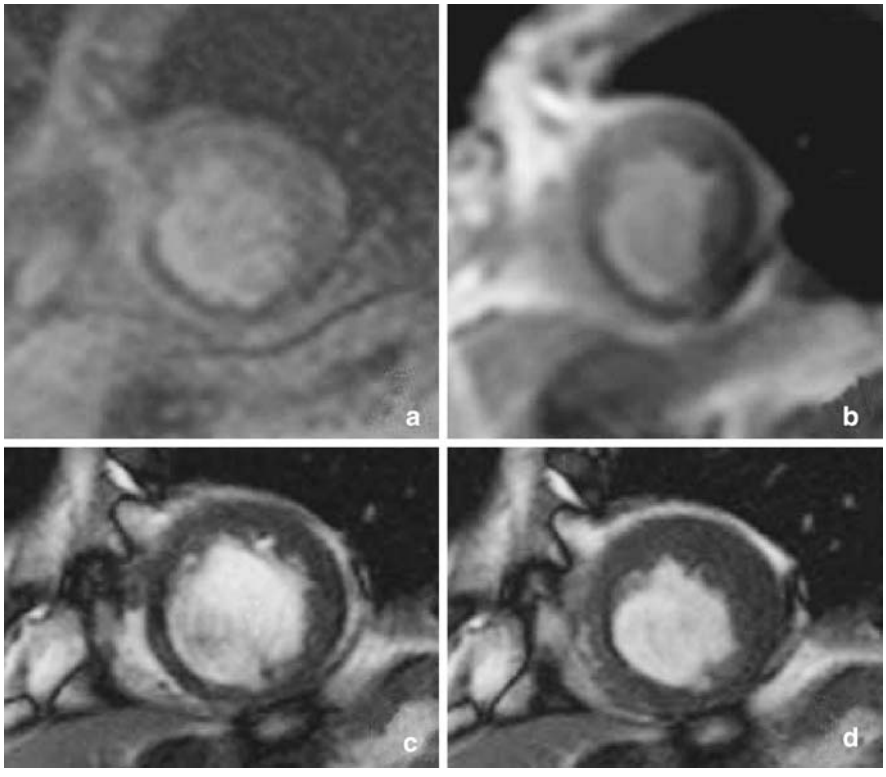

Fig. 7a–d Patient with a history of inferoseptal and inferior myocardial infarction; short-axis scan of the apical LV portion. The first-pass perfusion imaging (*top row*) during peak myocardial enhancement with **a** TurboFLASH and **b** TrueFISP shows a sharply demarcated perfusion defect in the inferoseptal and inferior segment. A lower signal of the lateral wall in the TrueFISP image is probably due to the signal inhomogeneity of the surface coil and does not correspond to a perfusion deficit. Note higher image noise and a foldover in the **a** TurboFLASH image. Cine SSFP images in **c** end-diastole and **d** end-systole show the akinesia in the inferior septum and the inferior segment

Differences between patients and volunteers

We found that volunteers had significantly higher SNR during peak enhancement in both TurboFLASH and TrueFISP. This effect is most probably related to the differences in bolus geometry. It has been shown that the concentration of contrast material is inversely proportional to the cardiac output; therefore, because of the depressed LV function in the patients with history of chronic myocardial infarction, a prolonged bolus of contrast material with consequently lower peak concentrations might cause lower SNR.

Clinical impact of MRI first-pass perfusion

A recently published study on the reliability of MRI-based perfusion imaging by Schwitter et al. showed a sensitivity of 85% and a specificity of 87% for the detection of coronary artery stenosis of more than 50% as defined by conventional coronary angiography [21]. Moreover, when comparing with ^{13}N ammonia PET as the clinical reference standard in perfusion imaging, even higher values, percentages above 95%, were found. Later, studies on stress-perfusion imaging using either Adenosine or Dipyridamol, yielded sensitivities between 72 and 92% and specificities between 78 and 97% for the detection of significant perfusion defects [6]. Based on these data, MRI-based first-pass perfusion imaging seems to offer reliable contributions to non-invasive diagnostics in CAD; however, there are still important limitations regarding SNR and temporal as well as spatial resolution.

Recently developed SSFP sequences are capable of a more sufficient use of the transverse magnetization through refocusing after data acquisition and adding with the newly generated transverse magnetization of the following phase-encoding step; therefore, SSFP has been shown to provide higher contrast while maintaining ultrashort repetition times [22]. These characteristics have put this technique into the view of cardiac MRI. They are being used for different applications and have replaced older GRE sequences. Numerous studies have reported the advantageous applications of SSFP in cardiac imaging [13, 14, 15, 23, 24, 25, 26]. Newer developments also allow for the use of SSFP in viability diagnostics. Consequently, myocardial first-pass perfusion imaging has been performed using SSFP sequences as their capabilities, such as short acquisition time and high contrast, are very useful with regard to this particular topic [27].

In the present study, patients with chronic myocardial infarction were examined with different sequences to evaluate the CNR between normally perfused myocardium and tissue with depressed perfusion such as chronic infarction scar. Although in clinical routine the perfusion of scar is not of interest, we used the myocardial infarction model to clarify the differences between both sequences. Whether the shown advantages of TrueFISP perfusion imaging will also apply in patients with ischemic but viable myocardium still needs to be confirmed in controlled studies.

Conclusion

Recently developed TrueFISP sequences provide better image quality and higher SNR and CNR in myocardial first-pass perfusion MR imaging and should, therefore, replace the established TurboFLASH techniques in this respect. A better delineation between ischemic and normally perfused myocardium through higher contrast-to-noise ratios might be suggested with TrueFISP. Larger controlled studies using stress perfusion protocols with Adenosine have to confirm this suggestion. In the future, the higher SNR values of TrueFISP sequences might allow the application of half-Fourier reconstruction or parallel acquisition techniques to improve temporal and spatial resolution.

References

1. Gibbons RJ, Abrams J, Chatterjee K, Daley J, Deedwania PC, Douglas JS, Ferguson TB Jr, Fihn SD, Fraker TD Jr, Gardin JM, O'Rourke RA, Pasternak RC, Williams SV, Alpert JS, Antman EM, Hiratzka LF, Fuster V, Faxon DP, Gregoratos G, Jacobs AK, Smith SC Jr (2003) ACC/AHA 2002 guideline update for the management of patients with chronic stable angina—summary article: a report of the American College of Cardiology/ American Heart Association Task Force on Practice Guidelines (Committee on the Management of Patients With Chronic Stable Angina). Circulation 107:149–158
2. Schwaiger M (1994) Myocardial perfusion imaging with PET. J Nucl Med 35:693–698
3. Go RT, Marwick TH, MacIntyre WJ, Saha GB, Neumann DR, Underwood DA, Simpfendorfer CC (1990) A prospective comparison of rubidium-82 PET and thallium-201 SPECT myocardial perfusion imaging utilizing a single dipyridamole stress in the diagnosis of coronary artery disease. J Nucl Med 31:1899–1905
4. Demer LL, Gould KL, Goldstein RA, Kirkeeide RL, Mullani NA, Smalling RW, Nishikawa A, Merhige ME (1989) Assessment of coronary artery disease severity by positron emission tomography: comparison with quantitative arteriography in 193 patients. Circulation 79:825–835
5. Manning WJ, Atkinson DJ, Grossman W, Paulin S, Edelman RR (1991) First-pass nuclear magnetic resonance imaging studies using gadolinium-DTPA in patients with coronary artery disease. J Am Coll Cardiol 18:959–965
6. Wilke NM, Jerosch-Herold M, Zenovich A, Stillman AE (1999) Magnetic resonance first-pass myocardial perfusion imaging: clinical validation and future applications. J Magn Reson Imaging 10:676–685

7. Keijer JT, van Rossum AC, van Eenige MJ, Bax JJ, Visser FC, Teule JJ, Visser CA (2000) Magnetic resonance imaging of regional myocardial perfusion in patients with single-vessel coronary artery disease: quantitative comparison with (201)Thallium-SPECT and coronary angiography. J Magn Reson Imaging 11:607–615
8. Lauerma K, Virtanen KS, Sipila LM, Hekali P, Aronen HJ (1997) Multislice MRI in assessment of myocardial perfusion in patients with single-vessel proximal left anterior descending coronary artery disease before and after revascularization. Circulation 96:2859–2867
9. Panting JR, Gatehouse PD, Yang GZ, Jerosch-Herold M, Wilke N, Firmin DN, Pennell DJ (2001) Echo-planar magnetic resonance myocardial perfusion imaging: parametric map analysis and comparison with thallium SPECT. J Magn Reson Imaging 13:192–200
10. Kraitchman DL, Chin BB, Heldman AW, Solaiyappan M, Bluemke DA (2002) MRI detection of myocardial perfusion defects due to coronary artery stenosis with MS-325. J Magn Reson Imaging 15:149–158
11. Schmitt M, Mohrs OK, Petersen SE, Kreitner KF, Voigtlander T, Wittlinger T, Horstick G, Ziegler S, Meyer J, Thelen M, Schreiber WG (2002) Evaluation of myocardial perfusion reserve in patients with CAD using contrast-enhanced MRI: a comparison between semiquantitative and quantitative methods. Rofo Fortschr Geb Rontgenstr Neuen Bildgeb Verfahr 174:187–195 [in German]
12. Wintersperger BJ, Penzkofer HV, Knez A, Weber J, Reiser MF (1999) Multislice MR perfusion imaging and regional myocardial function analysis: complimentary findings in chronic myocardial ischemia. Int J Card Imaging 15:425–434
13. Plein S, Bloomer TN, Ridgway JP, Jones TR, Bainbridge GJ, Sivananthan MU (2001) Steady-state free precession magnetic resonance imaging of the heart: comparison with segmented k-space gradient-echo imaging. J Magn Reson Imaging 14:230–236
14. Carr JC, Simonetti O, Bundy J, Li D, Pereles S, Finn JP (2001) Cine MR angiography of the heart with segmented true fast imaging with steady-state precession. Radiology 219:828–834
15. Barkhausen J, Hunold P, Jochims M, Eggebrecht H, Sabin GV, Erbel R, Debatin JF (2002) Comparison of gradient-echo and steady-state free precession sequences for 3D-navigator MR angiography of coronary arteries. Rofo Fortschr Geb Rontgenstr Neuen Bildgeb Verfahr 174:725–730 [in German]
16. Hunold P, Brandt-Mainz K, Freudenberg L, Vogt FM, Neumann T, Knipp S, Barkhausen J (2002) Evaluation of myocardial viability with contrast-enhanced magnetic resonance imaging: comparison of the late enhancement technique with positron emission tomography. Rofo Fortschr Geb Rontgenstr Neuen Bildgeb Verfahr 174:867–873 [in German]
17. Firbank MJ, Coulthard A, Harrison RM, Williams ED (1999) A comparison of two methods for measuring the signal-to-noise ratio on MR images. Phys Med Biol 44:N261–N264
18. Schreiber WG, Schmitt M, Kalden P, Horstick G, Gumbrich T, Petersen S, Mohrs O, Kreitner KF, Voigtlander T, Thelen M (2001) Perfusion MR imaging of the heart with TrueFISP. Rofo Fortschr Geb Rontgenstr Neuen Bildgeb Verfahr 173:205–210 [in German]
19. Schreiber WG, Schmitt M, Kalden P, Mohrs OK, Kreitner KF, Thelen M (2002) Dynamic contrast-enhanced myocardial perfusion imaging using saturation-prepared TrueFISP. J Magn Reson Imaging 16:641–652
20. Muhling OM, Dickson ME, Zenovich A, Huang Y, Wilson BV, Wilson RF, Anand IS, Seethamraju RT, Jerosch-Herold M, Wilke NM (2001) Quantitative magnetic resonance first-pass perfusion analysis: inter- and intraobserver agreement. J Cardiovasc Magn Reson 3:247–256
21. Schwitter J, Nanz D, Kneifel S, Bertschinger K, Buchi M, Knusel PR, Marincek B, Luscher TF, Schulthess GK von (2001) Assessment of myocardial perfusion in coronary artery disease by magnetic resonance: a comparison with positron emission tomography and coronary angiography. Circulation 103:2230–2235
22. Zur Y, Stokar S, Bendel P (1988) An analysis of fast imaging sequences with steady-state transverse magnetization refocusing. Magn Reson Med 6:175–193
23. Barkhausen J, Ruehm SG, Goyen M, Buck T, Laub G, Debatin JF (2001) MR evaluation of ventricular function: true fast imaging with steady-state precession vs fast low-angle shot cine MR imaging—feasibility study. Radiology 219:264–269
24. Foo TK, Ho VB, Marcos HB, Hood MN, Choyke PL (2002) MR angiography using steady-state free precession. Magn Reson Med 48:699–706
25. Spuentrup E, Bornert P, Botnar RM, Groen JP, Manning WJ, Stuber M (2002) Navigator-gated free-breathing three-dimensional balanced fast field echo (TrueFISP) coronary magnetic resonance angiography. Invest Radiol 37:637–642
26. Overall WR, Nishimura DG, Hu BS (2002) Fast phase-contrast velocity measurement in the steady state. Magn Reson Med 48:890–898
27. Klocke FJ, Simonetti OP, Judd RM, Kim RJ, Harris KR, Hedjbeli S, Fieno DS, Miller S, Chen V, Parker MA (2001) Limits of detection of regional differences in vasodilated flow in viable myocardium by first-pass magnetic resonance perfusion imaging. Circulation 104:2412–2416